

# Recrystallization Effects on Eco-Friendly Sol-Gel Spin-Coated TiO<sub>2</sub> Thin Films

Moniruzzaman Syed\*, Tawananyasha Karonga\* and Farhan Azim\*\*

\*Division of Natural and Mathematical Sciences, Lemoyne Owen College, Memphis, TN

Email: moniruzzaman\_syed@loc.edu

\*\* Department of Physics and Materials Science, University of Memphis, Memphis, TN

Email : mazim@memphis.edu

\*\*\*\*\*

## Abstract:

The increasing demand for high-efficiency solar cells has highlighted titanium dioxide (TiO<sub>2</sub>) thin films as a promising material for emerging photovoltaic technologies. In this study, TiO<sub>2</sub> thin films were deposited on silicon substrates using the sol-gel spin-coating technique, with hydrochloric acid (HCl) concentrations varied from 1 to 5 mL in the precursor solution. The films were subsequently annealed at 200°C and 500°C to investigate structural, optical, and morphological changes. Raman spectroscopy revealed a characteristic TiO<sub>2</sub> peak at 513 cm<sup>-1</sup> after annealing at 500°C, confirming recrystallization. XRD analysis identified anatase and rutile phases at  $2\theta = 33^\circ$  (110) and  $62^\circ$  (204), respectively, with crystallite sizes increasing from 51.13 nm at 200°C to 58.55 nm at 500°C. FTIR spectra showed Ti-O stretching bands near 600 and 750 cm<sup>-1</sup> for all samples. Surface analysis indicated improved homogeneity and increased roughness (up to 0.45  $\mu\text{m}$ ) with higher HCl volume at 500°C. UV-vis measurements demonstrated a reduction in direct band gap energy to 2.25-2.30 eV at 500°C. Ellipsometry results showed a decrease in film thickness with increasing HCl concentration, though overall thickness increased to approximately 3.3 nm at 500°C. The dielectric constant rose to values between 3 and 4, while the refractive index decreased from 3.7 to 3.3 with higher annealing temperature. These findings demonstrate the significant impact of acid concentration and thermal treatment on the properties of TiO<sub>2</sub> thin films, underscoring their strong potential for next-generation photovoltaic applications.

**Keywords — TiO<sub>2</sub> thin films, Sol-gel, Spin coating, Crystallization, Solar cell**

\*\*\*\*\*

## I. INTRODUCTION

Titanium dioxide (TiO<sub>2</sub>) thin films have garnered considerable attention in solar energy applications due to their excellent optical and electronic properties [1]. TiO<sub>2</sub> nanoparticles are cost-effective, chemically stable, and environmentally friendly, making them attractive for various technological uses. As a transparent conductive oxide (TCO), TiO<sub>2</sub> exhibits several remarkable characteristics, including a high refractive index [2], a large dielectric constant [3], and strong transparency in the visible region [4]. These features make TiO<sub>2</sub> particularly suitable for enhancing the efficiency of solar panels and other optoelectronic devices [5–6]. In addition, TiO<sub>2</sub> thin films are widely employed in

optical devices, refractory and wear-corrosion-resistant coatings, gas and biosensors, and other emerging applications.

The performance of TiO<sub>2</sub> thin films is strongly influenced by the deposition method and the interaction between the film and its substrate, such as glass or silicon [7]. These interactions affect nucleation, crystal formation, and particle size distribution. Multiple deposition techniques—including ion-beam deposition [8], chemical vapor deposition [9], evaporation [10], and magnetron sputtering [11] have been utilized to fabricate TiO<sub>2</sub> films. However, these methods often require expensive equipment and involve high operational and maintenance costs.

The sol-gel spin-coating technique has emerged as a preferred alternative due to its low cost, simplicity, scalability, and ability to produce uniform transparent thin films on various substrates, including silicon [12]. In this process, precursor chemistry plays a critical role in determining film quality. Titanium isopropoxide (TIP), a common precursor, undergoes rapid hydrolysis and polycondensation when mixed with water, often resulting in uncontrolled precipitation. This challenges the stability of the sol-gel process and limits film performance. The incorporation of hydrochloric acid (HCl) effectively moderates these reactions, stabilizing the solution and controlling the formation of molecular structures. Adjusting the concentration of HCl is therefore essential for tailoring film properties.

During high-temperature deposition on silicon substrates, an unintended SiO<sub>2</sub> interfacial layer may form, influencing the optical and electronic behavior of the TiO<sub>2</sub> film. Lower annealing temperatures are desirable to mitigate substrate damage, reduce interface reactions, and preserve film integrity. Proper heat treatment improves crystallinity by removing organic residues; however, insufficient heating may result in amorphous TiO<sub>2</sub> films. Typically, annealing temperatures near 400°C are required to achieve well-crystallized TiO<sub>2</sub> films through the sol-gel process.

In this study, TiO<sub>2</sub> thin films were deposited on silicon substrates using the sol-gel spin-coating technique, with varying HCl volume concentrations incorporated into the precursor solution to determine the optimum acid-water ratio. The films were annealed at 200°C and 500°C for 1 hour to evaluate the influence of thermal treatment on crystallinity. Raman spectroscopy, X-ray diffraction (XRD), ellipsometry, UV-Vis spectroscopy, FTIR, and topographic and surface roughness analyses were performed to investigate the structural and optical characteristics of the films. These evaluations were carried out to determine the suitability of sol-gel-derived TiO<sub>2</sub> thin films for next-generation high-efficiency solar cell applications.

## II. MATERIALS AND METHODS

### Substrate Cutting and Cleaning

Silicon substrates were cut into 10mm X 10 mm pieces using a diamond cutter. The substrates were then placed in separate beakers containing acetone, ethanol, and deionized (DI) water. Each beaker was subjected to ultrasonic cleaning for 15 minutes to remove organic and particulate contaminants.

### Precursor Chemicals

Titanium Isopropoxide {Ti[OCH(CH<sub>3</sub>)<sub>2</sub>]<sub>4</sub>}, Absolute Ethyl Alcohol (C<sub>2</sub>H<sub>5</sub>OH), Hydrochloric Acid (HCl), Deionized Water (H<sub>2</sub>O), and Silicon Substrates.

### Synthesis of TiO<sub>2</sub> Sol-Gel Solution

The TiO<sub>2</sub> sol-gel solution was prepared using the sol-gel synthesis technique. Titanium isopropoxide (TIP) was mixed with absolute ethyl alcohol (AEA) in a 1:2 volume ratio. To initiate hydrolysis, varying concentrations of hydrochloric acid (1, 2, 3, 4, and 5 mL) were separately mixed with 1 mL of deionized water. Each acid-water mixture was then added dropwise to the TIP-AEA solution under continuous magnetic stirring for 2 hours. This process facilitated sol-gel formation. After gelation, the solution was allowed to cool to room temperature before further processing.

### Thin Film Preparation

Double-sided adhesive tape was affixed to the surface of a large glass substrate, and the cleaned silicon substrates were positioned on the tape. The assembly was then placed inside the spin coater. The interior of the spin coater chamber was cleaned with acetone, and the device was connected to a vacuum pump. Once the vacuum was properly adjusted, the substrates adhered firmly to the spinning head.

A TiO<sub>2</sub> sol-gel solution prepared with 1 mL of HCl was deposited onto the silicon substrate using a dropper, with approximately 0.3 mL applied to each sample. The substrates were spun at 1000 rpm for 10 seconds to achieve uniform film spreading. The same deposition procedure was repeated for TiO<sub>2</sub> gels containing 2, 3, 4, and 5 mL of HCl. After each coating, the substrates were placed on a hot plate at

200°C for 1 hour to remove residual solvents and enhance film adhesion. This annealing process was subsequently repeated at 500°C to obtain the desired film thickness and crystalline structure. The resulting TiO<sub>2</sub> thin films were then prepared for further characterization.

### III. Thin Film Characterization

#### Raman Scattering

Raman spectroscopy was utilized to identify the crystalline phases of the TiO<sub>2</sub> thin films by observing their molecular vibrational modes. Raman analysis is particularly effective for distinguishing TiO<sub>2</sub> polymorphs due to its high sensitivity [13]. It is also suitable for thin films on silicon substrates, as shifts in Raman bands can indicate tensile or compressive strain during crystallographic changes. The prepared TiO<sub>2</sub> films were analyzed using a Quasar-TEC-X2 Raman spectrometer operating in the 200–2750 cm<sup>-1</sup> range, with a 785 nm excitation laser and 4 cm<sup>-1</sup> resolution. This non-destructive technique allows precise evaluation of surface structural properties.

#### X-Ray Diffraction (XRD)

XRD analysis provides insight into the crystallite size, phase composition, lattice spacing, and structural constants of TiO<sub>2</sub> thin films. It is used to determine whether the films are crystalline and to identify phases such as anatase, rutile, or brookite [14]. The average crystallite size was calculated using the Debye–Scherrer equation:

$$D = \frac{K\lambda}{\beta \cos \theta} \quad (1)$$

where  $K$  is the shape factor (~0.89),  $\lambda$  is the X-ray wavelength,  $\beta$  is the full width at half maximum (FWHM), and  $\theta$  is the Bragg angle.

Structural properties of the TiO<sub>2</sub>/silicon films were investigated using a Bruker D8 Advance X-ray diffractometer equipped with CuK $\alpha$  radiation ( $\lambda = 0.15406$  nm). Data were collected at 40 kV and 40

mA in the  $2\theta$  range of 20°–75°, with a step size of 0.0484° and a scan rate of 0.2°/s using a Ventec solid-state detector (Bruker, Germany)

#### Topographical Study

The surface morphology of the TiO<sub>2</sub> thin films was examined using a Portable Capture HD microscope (Version 3.0.1), allowing visualization of topographical features and uniformity across the film surface.

#### FT-IR Spectroscopy

FTIR spectroscopy was employed to identify functional groups and chemical bonds within the TiO<sub>2</sub> thin films. This technique provides insights into bonding environments, surface chemistry, and the presence of residual organic species. The Ti-O vibrational stretching and other chemical signatures of TiO<sub>2</sub>/Silicon films were analyzed using an MSE PRO Fourier Transform Infrared Spectrometer, with a spectral resolution of 1 cm<sup>-1</sup> and a measurement range of 375–7800 cm<sup>-1</sup>. FTIR is non-destructive and suitable for assessing both amorphous and crystalline films.

#### UV-Vis Measurements

UV-Vis spectroscopy was used to evaluate the optical properties of the TiO<sub>2</sub> thin films, including absorbance, transmittance, and reflectance. This technique is essential for estimating the optical band gap and understanding the film's light-matter interactions, which influence photocatalytic and photovoltaic performance. UV-Vis measurements were performed using a TF-C-UV-vis-SRN dual spectrometer system covering the 200–1700 nm wavelength range, with a resolution of <5 nm, using SL4 halogen and deuterium light sources and an R600 reflectance probe.

#### Surface Roughness Measurements

Surface roughness analysis provides quantitative information about film texture and uniformity, which can impact optical and electronic properties [15].

Roughness measurements were carried out using an SJ-310 Portable Surface Roughness Tester equipped with a retractable drive unit, a 4 mN detector, and a 5  $\mu\text{m}$  stylus tip radius.

## Ellipsometry Analysis

The film thickness and optical constants (refractive index and dielectric constant) of the  $\text{TiO}_2/\text{Silicon}$  films were determined using an FS-RT-300 multi-wavelength ellipsometer. Ellipsometry is a highly sensitive, non-destructive technique suitable for multilayer structures on reflective substrates such as silicon [16]. It enables accurate optical modeling and precise determination of thickness and optical interactions, which are essential for thin-film solar and optoelectronic applications.

## IV. RESULTS AND DISCUSSION

### Raman Scattering

Raman spectroscopy was employed to analyse the structural properties of  $\text{TiO}_2$  thin films deposited on silicon substrates, focusing on molecular vibrations and phase formation. At the annealing temperature of 200  $^\circ\text{C}$ , the films exhibited an amorphous nature, as indicated by weak and broad Raman signals (Fig. 1a), resulting in the absence of distinct  $\text{TiO}_2$  vibrational peaks. In contrast, annealing at 500  $^\circ\text{C}$  significantly improved crystallinity and phase development, demonstrated by the enhanced vibrational peak at 531.84  $\text{cm}^{-1}$  (Fig. 1b). Higher HCl concentrations during synthesis further contributed to sharper Raman features at 500  $^\circ\text{C}$ , suggesting improved phase purity and more ordered structural arrangement compared to the 200  $^\circ\text{C}$  films. These observations confirm the stabilization of the anatase phase through thermal treatment.

The improved crystallinity at elevated temperatures can be attributed to increased atomic mobility, enabling atoms within the  $\text{TiO}_2$  network to reorganize into a more ordered structure. Similar thermal recrystallization behavior in  $\text{TiO}_2$  films has been reported by Aarati Chacko et al. [17] and Mabkhoot A. Alsaiani et al., who observed enhanced

crystalline quality above 450  $^\circ\text{C}$  [18]. Additionally, slight red shifts in the Raman bands for both 200  $^\circ\text{C}$  and 500  $^\circ\text{C}$  annealed samples can be explained by inelastic (Stokes) scattering, where molecules return from excited states by emitting lower-energy photons with longer wavelengths. This red shift is also indicative of tensile strain within the  $\text{TiO}_2$  lattice, which promotes relaxation toward the anatase phase.

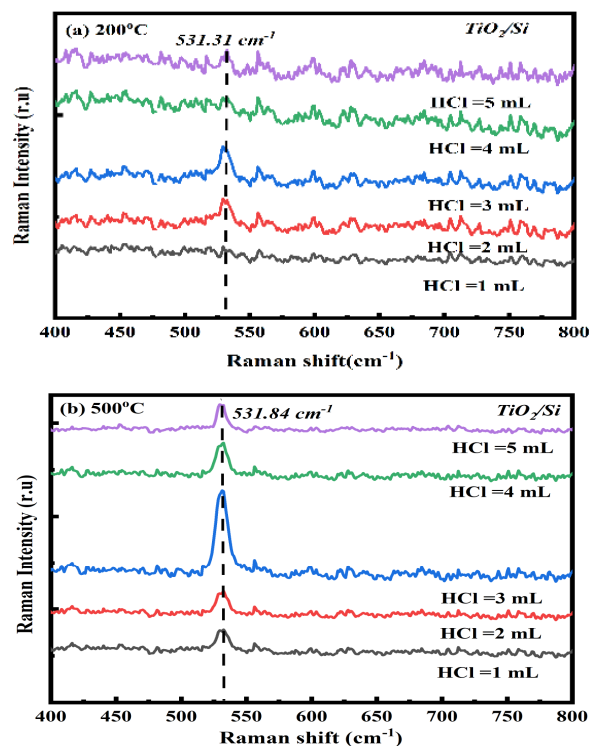


Fig. 1 Raman scattering analysis of the  $\text{TiO}_2$  thin films annealed at (a) 200 $^\circ\text{C}$  and (b) 500 $^\circ\text{C}$  temperatures

### X-Ray Diffraction

X-ray diffraction (XRD) analysis (Fig. 2a, b) confirmed the presence of both rutile and anatase phases in the  $\text{TiO}_2$  thin films, corresponding to Bragg angles near 33 $^\circ$  (110) and 62 $^\circ$  (204), respectively. Films annealed at 500  $^\circ\text{C}$  exhibited significantly higher crystallinity than those treated at 200  $^\circ\text{C}$  under identical HCl concentrations. The average crystallite sizes were determined using the Debye–Scherrer equation, and the results indicate a clear increase in crystallite size with higher annealing temperature, as shown in Fig. 2b. According to Fig. 2c, the crystallite size at 200  $^\circ\text{C}$  was approximately



52 nm for films treated with 2 mL of HCl, whereas it increased to about 58 nm when 5 mL of HCl was used at 500 °C. This progressive growth suggests that both annealing temperature and acid concentration significantly influence crystal development.

Similar observations were reported by Nicu Becherescu et al., who studied crystallite growth in TiO<sub>2</sub> under elevated thermal conditions [19], and by Jacek Nizioł et al., who documented phase evolution and increased crystallite size under comparable annealing treatments [20]. Higher volumes of HCl enhanced the hydrolysis rate during the sol-gel process, leading to improved nucleation and crystal formation. Furthermore, annealing at 500 °C promoted densification and increased thermodynamic stability of the films by reducing structural defects. This facilitated the merging of small crystalline domains, ultimately resulting in larger crystallite sizes.

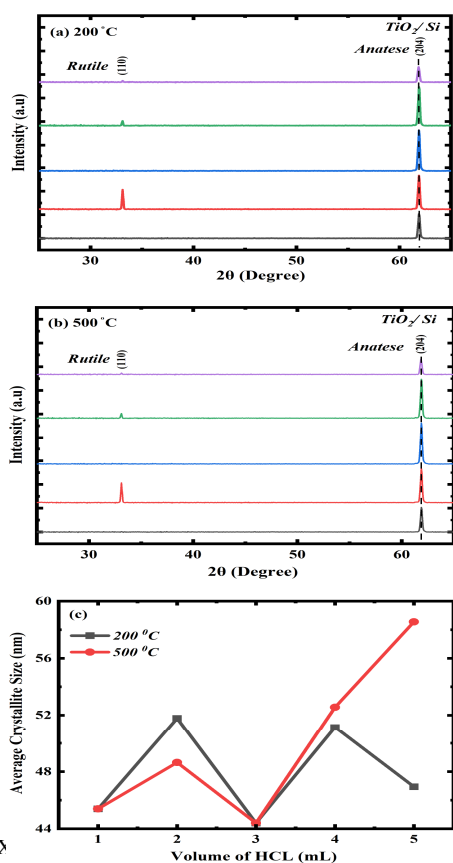


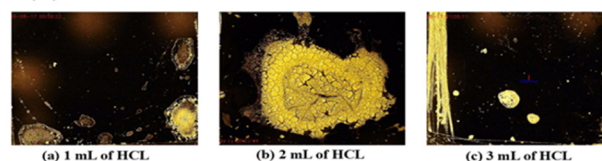
Fig. 2 (a) 200 °C, (b) 500 °C, and (c) average crystallite size concerning different volume concentrations of HCl acid mixture at both annealed temperatures.

### Topographic Study

The morphological analysis presented in Fig. 3.1(a–e) shows that the films annealed at 200 °C exhibited smoother surfaces with finer grains, suggesting a predominantly amorphous structure at lower temperatures. In contrast, the films annealed at 500 °C, as shown in Fig. 3.2(a–e), demonstrated improved homogeneity and a more uniform grain distribution. The elevated annealing temperature facilitated recrystallization and enhanced surface texturing. Signs of rapid nucleation were evident through grain clustering, particularly at higher HCl concentrations. Overall, the surface topography confirms that annealing temperature strongly influences the structural and morphological evolution of the TiO<sub>2</sub> thin films.

### 3.1

#### (a) Annealed at 200 °C



### 3.2

#### (b) Annealed at 500 °C

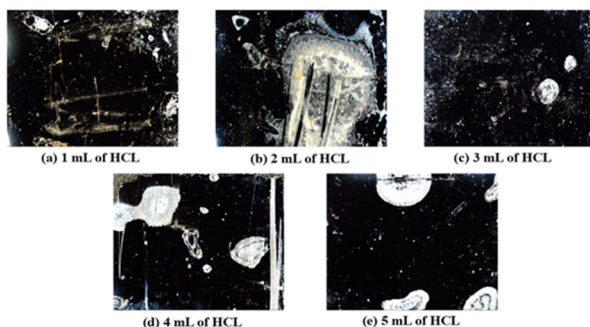


Fig. 3 Morphological study of the TiO<sub>2</sub> thin films annealed at (a) 200 °C and (b) 500 °C temperatures

### FT-IR Spectroscopy

Fourier Transform Infrared (FTIR) spectroscopy, shown in Fig. 4 (a, b), was employed to identify the chemical bonding and functional groups present in the TiO<sub>2</sub> thin films. Characteristic transmittance

peaks confirmed the vibrational modes of Ti–O-related bonds, including the Ti–O stretching band near  $600\text{ cm}^{-1}$  and the Ti–O–Ti bridging vibration around  $750\text{ cm}^{-1}$  [21]. The stretching band observed at approximately  $970\text{ cm}^{-1}$  corresponds to Si–O–Ti bonding, indicating strong interfacial interaction between the  $\text{TiO}_2$  film and the silicon substrate. A peak near  $900\text{ cm}^{-1}$  was attributed to C–C bonding, likely originating from residual isopropyl alcohol (IPA) used during the sol–gel precursor preparation.

Additional minor peaks detected in the  $1000\text{--}1500\text{ cm}^{-1}$  region can be attributed to bending vibrations of C–N or C–O functional groups. Transmittance features between  $1500\text{--}2000\text{ cm}^{-1}$  were associated with stretching vibrations of double bonds such as C=O, C=C, and C=H. Furthermore, broad absorption features between  $2750\text{--}3750\text{ cm}^{-1}$  were attributed to O–H, N–H, and C–H stretching, likely originating from ambient moisture or residual hydroxyl groups on the film surface.

Similar FTIR features have been reported by Sebastián Alberti et al., confirming the persistence of these functional groups across different annealing conditions [22]. The absence of strong organic impurity peaks suggests effective decomposition of residual solvents and precursors, confirming the chemical purity and integrity of the sol–gel-derived  $\text{TiO}_2$  thin films.

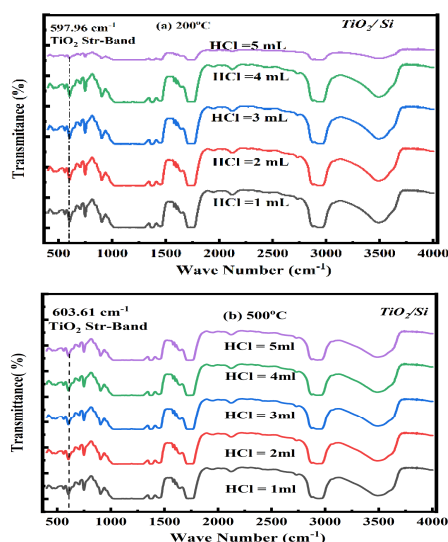


Fig. 4 FTIR spectroscopy analysis of the  $\text{TiO}_2$  thin films annealed at (a)  $200^\circ\text{C}$  and (b)  $500^\circ\text{C}$  temperatures.

## UV-Vis Measurements

UV-Vis spectroscopy of  $\text{TiO}_2$  thin films annealed at  $200^\circ\text{C}$  and  $500^\circ\text{C}$  is presented in Fig. 5 (a, b). The films exhibited strong absorption in the UV region, centered around  $290\text{--}300\text{ nm}$ , with higher acid concentrations resulting in increased absorbance intensity. This enhancement is attributed to the accelerated hydrolysis rate at elevated HCl concentrations during the sol-gel process, which promotes the formation of well-dispersed nanoparticles and a more homogeneous film surface, thereby improving light absorption.

The optical band gap energies of the films were determined from Tauc plots derived from the UV–Vis spectra [23], assuming a direct transition ( $n = 2$ ) based on linear fitting. As the annealing temperature increased from  $200^\circ\text{C}$  to  $500^\circ\text{C}$ , the band gap decreased from  $3.07\text{ eV}$  to  $2.28\text{ eV}$  (Fig. 5c), indicating a narrowing of the energy gap between the valence and conduction bands. This reduction reflects enhanced electronic transition behavior, which is associated with improved crystallinity and densification of the films at higher temperatures. In particular,  $\text{TiO}_2$  films annealed at  $500^\circ\text{C}$  with  $5\text{ mL}$  HCl exhibited higher crystallinity and denser surface morphology, which may reduce quantum confinement effects and contribute to the observed band gap narrowing [24].

The measured band gap values ( $2.28\text{--}3.07\text{ eV}$ ) are consistent with the reported range for  $\text{TiO}_2$  ( $3\text{--}3.2\text{ eV}$ ) and remain significantly higher than that of silicon ( $\sim 1.2\text{ eV}$ ), making these  $\text{TiO}_2/\text{Si}$  films suitable for solar cell applications. Maintaining a moderately wide band gap is critical, as excessively low band gap energies can lead to increased heat generation due to excessive light absorption, which may degrade the material properties and performance of the photovoltaic device.

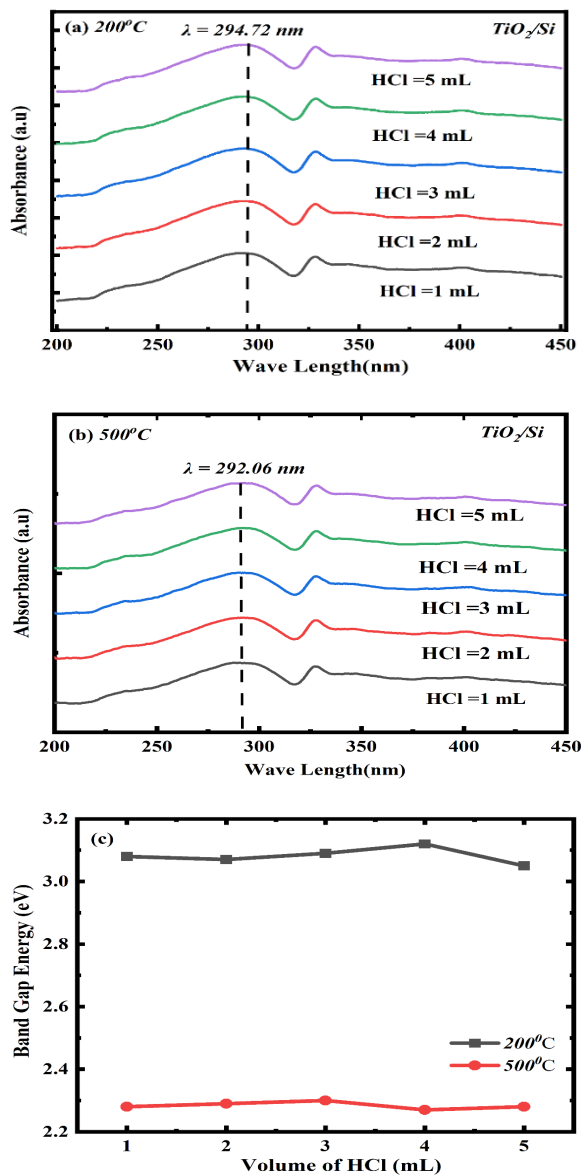


Fig. 5 UV vis spectroscopy analysis of the TiO<sub>2</sub> thin films annealed at (a) 200°C, (b) 500°C, and (c) band gap energy concerning different volume concentrations of HCl acid mixture at both annealed temperatures.

### Surface Roughness

Surface roughness measurements of the TiO<sub>2</sub> thin films are presented in Fig. 6. Films annealed at 200 °C exhibited relatively smooth and uniform surfaces, whereas those treated at 500 °C showed increased surface roughness accompanied by particle clustering. The maximum roughness values were measured as 0.32  $\mu\text{m}$  for films with 2 mL HCl at 200 °C and 0.45  $\mu\text{m}$  for films with 5 mL HCl at 500 °C. This increase in roughness can be attributed

to enhanced grain growth and recrystallization at elevated temperatures, particularly under higher HCl concentrations.

Similar trends have been reported by Yang Liu et al., who investigated morphological changes in annealed TiO<sub>2</sub> films [25], and by Joydip Sengupta et al., who observed surface texture transformations between low- and high-temperature-processed TiO<sub>2</sub> thin films [26]. In photovoltaic applications, such as solar cells, the increased surface roughness can be advantageous, as it provides greater grain exposure and surface area, enhancing interfacial interactions and potentially improving device performance.

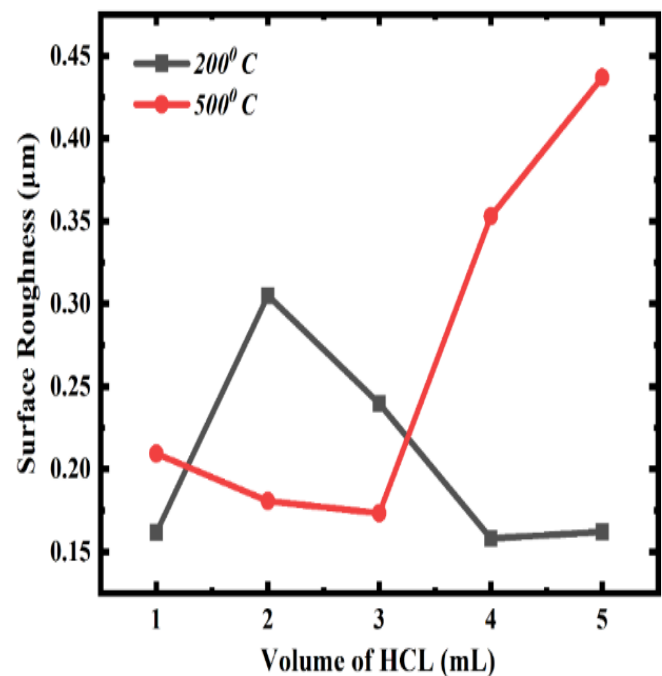


Fig. 6 Surface roughness analysis of the TiO<sub>2</sub> thin films annealed at 200°C and 500°C temperatures, concerning different volume concentrations of HCl acid mixture.

### Ellipsometer Analysis

Ellipsometry results, shown in Fig. 7(a), indicate that annealing led to a modest decrease in the refractive index of the TiO<sub>2</sub> thin films. The refractive index decreased with increasing annealing temperature, with films treated at 500 °C exhibiting lower values compared to those annealed at 200 °C. Specifically, the lowest refractive index was 3.7 for 3 mL HCl at 200 °C and 3.3 for 2 mL HCl at 500 °C.

This decrease suggests that higher annealing temperatures and greater HCl concentrations promote densification and hardening of the films, reflecting improved crystallinity, reduced porosity, and enhanced overall film quality.

Dielectric constants, presented in Fig. 7(b), were significantly higher for films annealed at 500 °C, ranging from 3 to 4, compared to 0–0.5 at 200 °C across different HCl concentrations. The nearly linear trend observed in the dielectric response indicates that variations in HCl concentration had a minimal effect on dielectric properties. The enhanced dielectric constant at elevated temperatures is attributed to improved material ordering and higher film density, which facilitates polarization under an electric field. This, in turn, strengthens local electric fields, improving charge separation efficiency—a critical parameter for solar cell applications. The optical constants suggest that the TiO<sub>2</sub> films behave as n-type semiconductors and, when combined with p-type silicon substrates, form a P–N junction capable of efficient electron–hole separation under illumination.

Figure 7(c) shows the variation of TiO<sub>2</sub> film thickness with HCl concentration. At 500 °C, thickness strongly influenced the optical and structural properties, with thicker films exhibiting enhanced crystallinity and reduced band gap energies [27]. The maximum thickness values were 3.3 nm at 200 °C for 2 mL HCl and 5.4 nm at 500 °C for 1 mL HCl. The increase in thickness at higher annealing temperature is attributed to thermal oxidation of the TiO<sub>2</sub> films in conjunction with the silicon substrate, leading to densification and growth of the crystalline layer. Thicker films provide more active surface sites and improved light absorption, enhancing the suitability of the TiO<sub>2</sub> thin films for photovoltaic applications [28].

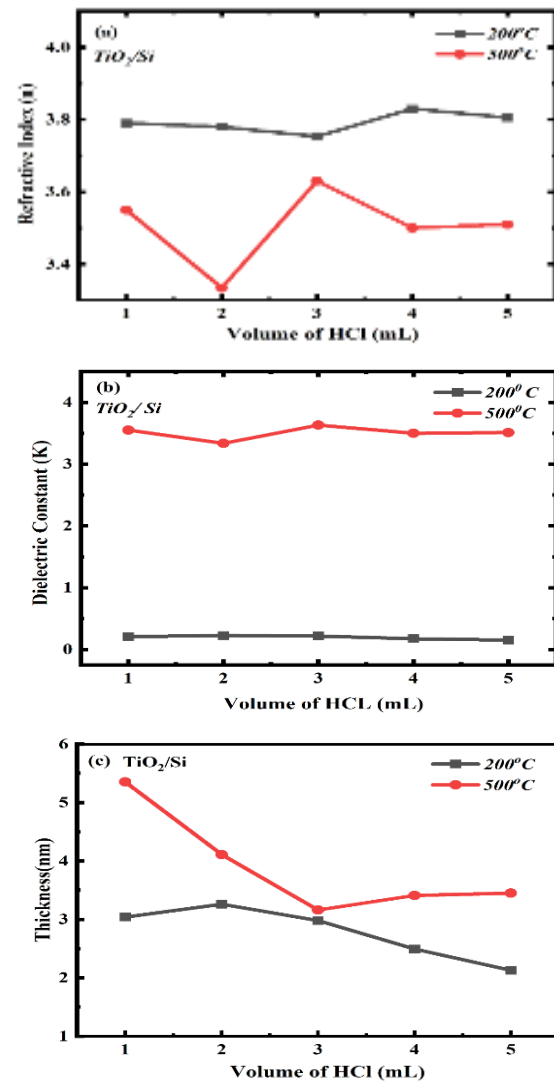


Fig.7 Characterization of (a) refractive index, (b) dielectric constant, and (c) thickness of the TiO<sub>2</sub> thin films annealed at 200°C and 500°C, concerning different volume concentrations of HCl acid mixture at both annealed temperatures.

## V. CONCLUSION

Titanium dioxide (TiO<sub>2</sub>) thin films were successfully deposited on silicon substrates via a facile sol-gel spin coating technique. Different molar concentrations of HCl were incorporated into the precursor solutions to investigate the effect of acid concentration on film properties. Subsequent annealing at 200 °C and 500 °C had a significant impact on the structural, optical, and surface characteristics of the films. At 200 °C, the films exhibited partial crystallization and moderate surface roughness, indicating initial phase formation and limited grain growth. Increasing the annealing



temperature to 500 °C enhanced the maximum crystallite size from 51.13 nm to 58.55 nm and increased the surface roughness from 0.32 µm to 0.45 µm, reflecting improved structural ordering and reduced defect density. The optical band gap decreased from 3.07 eV at 200 °C to 2.28 eV at 500 °C, indicating improved electronic conductivity. Moreover, the refractive index decreased to 3.3, while the dielectric constant increased to 3–4 at 500 °C, demonstrating enhanced optical properties. Overall, heat treatment at 500 °C significantly improved the crystallinity, surface uniformity, and optical performance of TiO<sub>2</sub>/Si thin films, highlighting its effectiveness in optimizing film quality for next-generation high-efficiency solar cell applications.

## ACKNOWLEDGMENT

The authors gratefully acknowledge the support of the U.S. Department of Education through the MSEIP Grant (#P120A220064) at LeMoyne-Owen College. Special thanks are extended to the Department of Physics at the University of Memphis, TN, for their assistance with XRD measurements. The authors also wish to express their sincere appreciation to Dr. Lisa Lang for her invaluable support of the research conducted at LeMoyne-Owen College.

## REFERENCES

- [1] Y Liang, et al. 2018, "The preparation of TiO<sub>2</sub> film by the Sol-Gel method and evaluation of its Self-Cleaning property," *Materials*, vol. 11, no. 3, p. 450
- [2] T Fuyuki & H Matsunami, 1986, "Electronic Properties of the Interface between Si and TiO<sub>2</sub> Deposited at Very Low Temperatures," *Japanese Journal of Applied Physics*, vol. 25, no. 9R, p. 1288
- [3] J-Y Gan, YC Chang & Wu, TB 1998, "Dielectric property of (TiO<sub>2</sub>)<sub>x</sub>-(Ta<sub>2</sub>O<sub>5</sub>)<sub>1-x</sub> thin films," *Applied Physics Letters*, vol. 72, no. 3, pp. 332–334
- [4] HK Pulker, 1979, "Characterization of optical thin films," *Applied Optics*, vol. 18, no. 12, p. 1969
- [5] Linse Bigler, AL, Lu, G., & Yates, J.T. 1995, "Photocatalysis on TiO<sub>2</sub> surfaces: principles, mechanisms, and selected results," *Chemical Reviews*, vol. 95, no. 3, pp. 735–758
- [6] M Kumar, M Kumar, & D Kumar, 2009, "The deposition of nanocrystalline TiO<sub>2</sub> thin film on silicon using Sol-Gel technique and its characterization," *Microelectronic Engineering*, vol. 87, no. 3, pp. 447–450
- [7] B Kraeutler & AJ Bard 1978, "Heterogeneous photocatalytic decomposition of saturated carboxylic acids on titanium dioxide powder. Decarboxylative route to alkanes," *Journal of the American Chemical Society*, vol. 100, no. 19, pp. 5985–5992
- [8] L J Meng & MPD Santos, 1993, "Investigations of titanium oxide films deposited by d.c. reactive magnetron sputtering in different sputtering pressures," *Thin Solid Films*, vol. 226, no. 1, pp. 22–29
- [9] GA Battiston, et al. 1996, "Chemical vapour deposition and characterization of gallium oxide thin films," *Thin Solid Films*, vol. 279, no. 1–2, pp. 115–118
- [10] P Löbl, M Huppertz & D Mergel 1994, "Nucleation and growth in TiO<sub>2</sub> films prepared by sputtering and evaporation," *Thin Solid Films*, vol. 251, no. 1, pp. 72–79
- [11] N Martin et al. 1996, "Characterizations of titanium oxide films prepared by radio frequency magnetron sputtering," *Thin Solid Films*, vol. 287, no. 1–2, pp. 154–163
- [12] CJ Brinker & Harrington 1981, "Sol-gel derived antireflective coatings for silicon," *Solar Energy Materials*, vol. 5, no. 2, pp. 159–172
- [13] M. Syed, B. Preyer, S. Velasquez, M. Syeda, J. Sultana, F. Azim. (2025). Substrate Dependency of Nucleation Mechanism in the formation of TiO<sub>2</sub> Thin Films by Sol-gel Spin-Coating Method. In *International Journal of Scientific Research and Engineering Development* (Vol. 8, Number 2, pp. 496–506). Zenodo.
- [14] M Syed, et al. 2025, "Sol-Gel derived CDO: AL thin films on various substrates: a comprehensive study on structural, morphological, optical, and electrical properties," *Journal of Materials Science Research*, vol. 14, no. 1, p. 22
- [15] M. Syeda, M. Syed, J. Massey, K. Harvey, M. Hurd, J. Sultana, F. Azim. (2024). Structural and Optical Properties of Aluminium Doped Cadmium Oxide (CdO: Al) Thin Film Prepared by Sol-Gel Spin-Coating Method. In *IJSRED - International Journal of Scientific Research and Engineering Development* (Vol. 7, Number 4, pp. 773–785). Zenodo.
- [16] M Syed et al. 2024, "Structural and electronic impact on various substrates of TiO<sub>2</sub> thin film using Sol-Gel spin coating method," *Journal of Materials Science Research*, vol. 13, no. 2, p. 1
- [17] Chacko, A et al. 2025, "On tailoring structural and optoelectronic properties of TiO<sub>2</sub> thin films synthesized via 'room' temperature high power impulse magnetron sputtering (Hip IMS)," *Journal of Physics Energy*,
- [18] Alsaiani, MA et al. 2020, "Growth of amorphous, anatase and rutile phase TiO<sub>2</sub> thin films on Pt/TiO<sub>2</sub>/SiO<sub>2</sub>/Si (SSTOP) substrate for resistive random-access memory (ReRAM) device application," *Ceramics International*, vol. 46, no. 10, pp. 16310–16320
- [19] Nizioł, J et al. 2024b, "Demonstration of the optical isotropy of TiO<sub>2</sub> thin films prepared by the Sol-Gel Method," *Materials*, vol. 17, no. 14, p. 3391
- [20] Simionescu, O-G et al. 2019, "RF magnetron sputtering deposition of TiO<sub>2</sub> thin films in a small continuous oxygen flow rate," *Coatings*, vol. 9, no. 7
- [21] Fujita, S, & Inagaki, S 2008, "Self-Organization of Organosilica Solids with Molecular-Scale and Mesoscale Periodicities," *Chemistry of Materials*, vol. 20, no. 3, pp. 891–908
- [22] Richards, BS et al. 2004, "High temperature processing of TiO<sub>2</sub> thin films for application in silicon solar cells," *Journal of Vacuum Science & Technology a: Vacuum Surfaces and Films*, vol. 22, no. 2, pp. 339–348
- [23] Alberti, S, & Jágerská, J 2021b, "Sol-Gel Thin film processing for integrated waveguide sensors," *Frontiers in Materials*, vol. 8
- [24] Galogahi, FM et al. 2020, "Core-shell microparticles: Generation approaches and applications," *Journal of Science Advanced Materials and Devices*, vol. 5, no. 4, pp. 417–435
- [25] Sengupta, J et al. 2011, "Influence of annealing temperature on the structural, topographical and optical properties of sol-gel derived ZnO thin films," *Materials Letters*, vol. 65, no. 17–18, pp. 2572–2574
- [26] Liu, Y et al. 2024, "Sol-gel synthesis of tetragonal BaTiO<sub>3</sub> thin films under fast heating," *Applied Surface Science*, vol. 661, p. 160086
- [27] Abed, A., & Al-Mathloom, A. 2019, "Titanium dioxide thin film prepared by Sol-Gel technique," *Journal of College of Education for Pure Science*, vol. 9, no. 1, pp. 241–258
- [28] Danks, AE, Hall, SR, & Schnepf, Z. 2015, "The evolution of 'sol-gel' chemistry as a technique for materials synthesis," *Materials Horizons*, vol. 3, no. 2, pp. 91–112